AIP Applied Physics Letters

# Oxide thinning percolation statistical model for soft breakdown in ultrathin gate oxides

Ming-Jer Chen, Ting-Kuo Kang, Chuan-Hsi Liu, Yih J. Chang, and Kuan-Yu Fu

Citation: Applied Physics Letters **77**, 555 (2000); doi: 10.1063/1.127042
View online: http://dx.doi.org/10.1063/1.127042
View Table of Contents: http://scitation.aip.org/content/aip/journal/apl/77/4?ver=pdfcov
Published by the AIP Publishing

**Articles you may be interested in**

Characterization of breakdown in ultrathin oxides by hot carrier emission
Appl. Phys. Lett. **84**, 4641 (2004); 10.1063/1.1759383

Unified model for breakdown in thin and ultrathin gate oxides (12–5 nm)
J. Appl. Phys. **86**, 5131 (1999); 10.1063/1.371489

Non-Gaussian behavior and anticorrelations in ultrathin gate oxides after soft breakdown
Appl. Phys. Lett. **74**, 1579 (1999); 10.1063/1.123622

Model for the current–voltage characteristics of ultrathin gate oxides after soft breakdown
J. Appl. Phys. **84**, 4351 (1998); 10.1063/1.368654

Soft breakdown in ultrathin gate oxides: Correlation with the percolation theory of nonlinear conductors
Appl. Phys. Lett. **73**, 514 (1998); 10.1063/1.121918

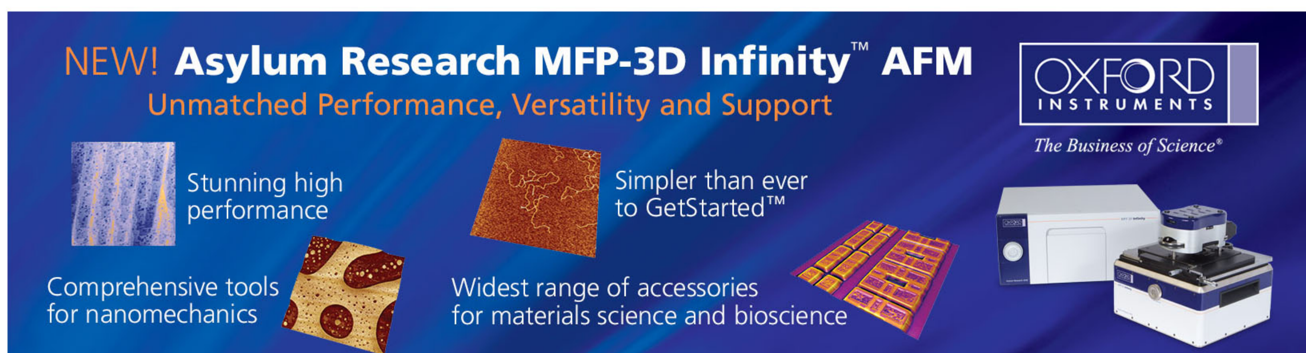


This article is copyrighted as indicated in the article. Reuse of AIP content is subject to the terms at: http://scitation.aip.org/termsconditions. Downloaded to IP: 140.113.38.11 On: Thu, 01 May 2014 07:46:44

# Oxide thinning percolation statistical model for soft breakdown in ultrathin gate oxides

Ming-Jer Chen[a] and Ting-Kuo Kang
*Department of Electronics Engineering, National Chiao-Tung University, Hsin-Chu, Taiwan, Republic of China*

Chuan-Hsi Liu, Yih J. Chang, and Kuan-Yu Fu
*United Microelectronics Corporation (UMC), Science-Based Industrial Park, Hsin-Chu, Taiwan, Republic of China*

(Received 3 February 2000; accepted for publication 31 May 2000)

An existing cell-based percolation model with parameter correlation can find its potential applications in assessing soft-breakdown (BD) statistics as long as the oxide thinning due to the localized physical damage near the $SiO_2/Si$ interface is accounted for. The resulting model is expressed explicitly with the critical trap number per cell $n_{BD}$ and the remaining oxide thickness $t'_{ox}$ both as parameters. Reproduction of time-to-bimodal (soft- and hard-) breakdown statistical data from 3.3-nm-thick gate-oxide samples yields $n_{BD}$ of 3 and 4 for soft and hard breakdown, respectively. The extracted $t'_{ox}$ of 1.0 nm for soft breakdown, plus the transition layer thickness of 0.5 nm in the model, is fairly comparable with literature values from current–voltage fitting. The dimension and area of the localized physically damaged region or percolation path (cell) are quantified as well. Based on the work, the origins of soft and hard breakdown are clarified in the following: (i) soft breakdown behaves intrinsically as hard breakdown, that is, they share the same defect (neutral trap) generation process and follow Poisson random statistics; (ii) both are independent events corresponding to different $t'_{ox}$ requirements; and (iii) hard breakdown takes place in a certain path located differently from that for the first soft breakdown. © *2000 American Institute of Physics.* [S0003-6951(00)02130-6]

The time-dependent dielectric breakdown is one of the most issues of concern in scaled metal–oxide–semiconductor field-effect transistors (MOSFETs). An anomalous phenomenon of soft breakdown (SBD) (also called *B*-mode stress-induced leakage current[1] and quasibreakdown),[2] which behaves fundamentally differently from hard breakdown (HBD), has recently been observed in ultrathin (<5 nm) gate oxides.[1–7] The oxide thinning theory[2] has originally been reported in explaining this phenomenon: the electrons injected from the polysilicon gate can travel through the ultrathin oxide ballistically and release most of their energy to physically damage the anode $SiO_2/Si$ interface, thus effectively reducing the oxide thickness to the direct tunneling regime. This theory has been cited in many applications such as post-soft-breakdown current–voltage ($I-V$) models,[2,8,9] quantitative determination of the remaining oxide thickness by $I-V$ fitting,[2,9] and physics basis for electron and hole direct tunneling conduction.[10] On the other hand, there have been published a series of percolation statistical models each successfully dealing with dielectric breakdown.[11–15] In this letter, we demonstrate that a cell-based percolation model with parameter correlation[15] can find potential applications in assessing soft-breakdown statistics as long as the local oxide thinning[2] is accounted for. In such a way, current understandings regarding the origins of soft and hard breakdown, the dimension and area of the localized physically damaged region, and the remaining oxide thickness, can all be substantially improved.

The $n$-channel MOSFETs with two different gate-oxide areas of $50\times50$ and $80\times100\ \mu m^2$ were fabricated in a 0.18 $\mu$m process. In this process, the gate oxide was thermally grown in a dilute oxygen ambient, and the polysilicon gate was arsenic implanted at 50 keV and $2\times10^{15}\ cm^{-2}$, followed by $N_2O$ annealing. The gate-oxide thickness $t_{ox}$ was determined to be 3.3 nm by polysilicon depletion and quantum-mechanical-corrected $C-V$ method. Stressing gate oxide was carried out under gate electron injection with constant current $J_G$ of $-125$ mA/cm$^2$ and with source, drain, and substrate tied to ground. The variation of gate voltage with stress time was monitored, from which the two key time criteria were extracted, namely, the time to soft breakdown $T_{SBD}$ and the time to hard breakdown $T_{HBD}$. Figure 1 depicts the measured results by HP4145B for two typical samples, respectively, showing the presence of bimodal (both soft and hard) breakdown and the absence of soft breakdown. At $T_{SBD}$ a first, small sudden drop of around 20 mV in gate voltage occurred while a more drastic change down to around $-1$ V was observed at $T_{HBD}$. It was found that about 95% of the total samples exhibit bimodal characteristics, whereas the remaining show only hard breakdown, that is, no noticeable signal for soft breakdown can be detected, as explained later. The inset of Fig. 2 shows the experimental $T_{SBD}$ and $T_{HBD}$ distributions from all samples in a Weibull plot, revealing that as hard breakdown turns into soft breakdown, the modal of the distributions moves to a lower time scale and the Weibull slope decreases. Also plotted in Fig. 2

[a]Electronic mail: mjchen@rpl.ee.nctu.edu.tw

This article is copyrighted as indicated in the article. Reuse of AIP content is subject to the terms at: http://scitation.aip.org/termsconditions. Downloaded to IP: 140.113.38.11 On: Thu, 01 May 2014 07:46:44

 © 2000 American Institute of Physics

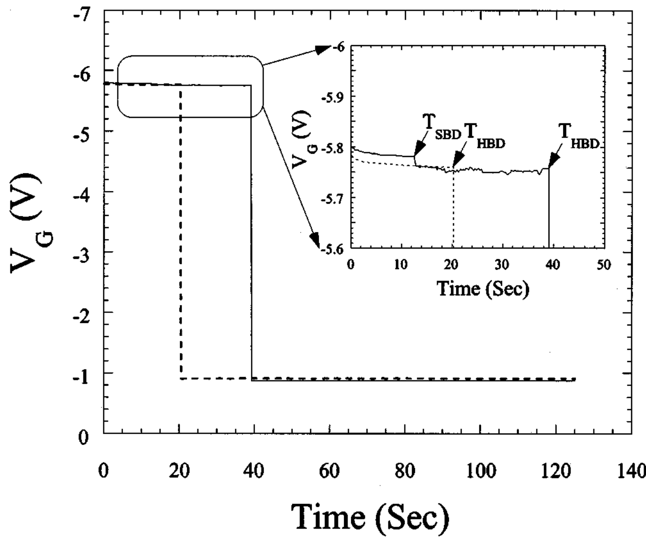


FIG. 1. Measured gate voltage vs stress time under constant current stressing for two samples. The oxide area was $80\times100\ \mu m^2$ and the stressing was done in gate injection of $-125\ mA/cm^2$.

is the Weibull plot translated to the oxide area $A_{ox}$ of $80\times100\ \mu m^2$ using Poisson area scaling,[16] showing that both soft and hard breakdown indeed follow Poisson random statistics.[17]

The above time-to-breakdown parameters $T_{SBD}$ and $T_{HBD}$ were defined in terms of different sudden drops in gate voltage. This definition is adequate since it was found that after $T_{SBD}$ the poststress gate $I-V$ characteristic curve resembled the direct tunneling one of the fresh oxide with thinner thickness as reported earlier,[2,3,9,10] while it became Ohmic after $T_{HBD}$. In addition, three relevant observations were drawn from emission spectroscopy EMMI pictures (not shown here): (i) the number of photoemission sites for soft breakdown increases with stress time; (ii) these sites were randomly distributed; and (iii) the first soft-breakdown site was different from the hard-breakdown site. Indeed, we measured electrically several soft-breakdown events prior to the

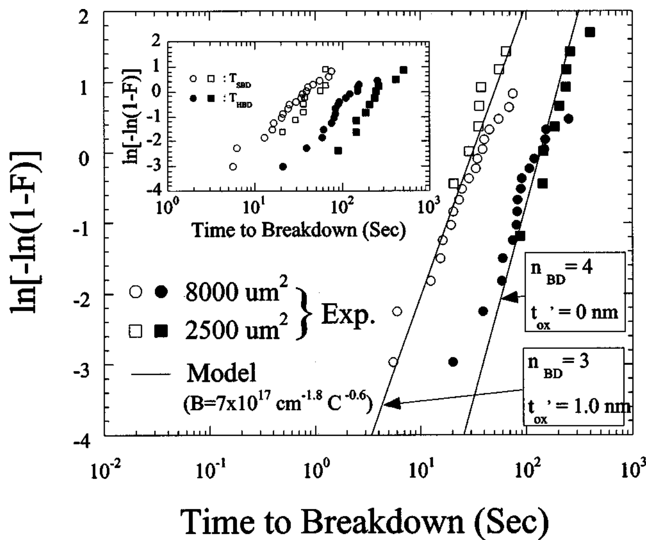


FIG. 2. Translated (with respect to $80\times100\ \mu m^2$) statistical distributions of time to soft breakdown $T_{SBD}$ and time to hard breakdown $T_{HBD}$. Also plotted are the lines from the model. The inset shows $T_{SBD}$ and $T_{HBD}$ distributions for two oxide areas.

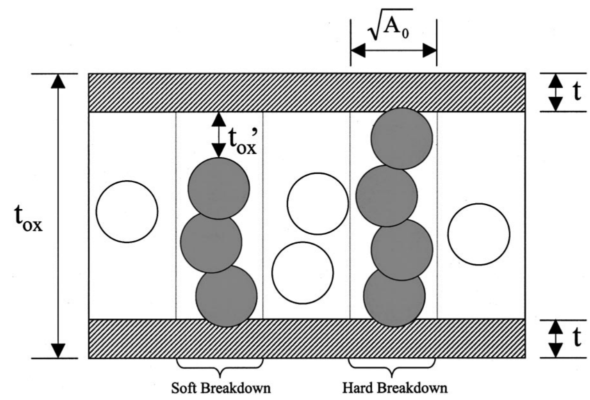


FIG. 3. Cross-sectional schematic showing a localized oxide thinning percolation path and a hard-breakdown percolation path. The spheres represent the traps generated during stress. The figure is not to scale.

final hard breakdown. Further evidence was found by plotting a scatter diagram (not shown here) between the measured $T_{SBD}$ and $T_{HBD}$ from the above 95% of the samples, exhibiting a very weak correlation between soft breakdown and hard breakdown. This suggests both events are statistically independent of each other.

Dielectric breakdown can be regarded as a process of the neutral electron trap generation during stress, critically producing one percolation path or more. The gate-oxide area can be divided into many identical square cells with cell area $A_0$.[11,12] Figure 3 schematically shows two different percolation paths within the cell, respectively, representing soft and hard breakdown. In the hard-breakdown percolation path, the traps span the whole oxide to connect one plate to the other one, while for the soft-breakdown path such plate-to-plate connection is incomplete as characterized by the remaining oxide thickness $t'_{ox}$ over the localized physically damaged region according to the theory.[2] Obviously, all the traps are randomly generated within the effective thickness of $t_{ox}-2t-t'_{ox}$ for soft breakdown. Here, $t(=0.5\,nm)$ (Refs. 14 and 15) denotes the transition-layer thickness to account for the conductive nature in the vicinity of the interface between the polysilicon gate and oxide and that between the oxide and underlying silicon. The critical trap density $N_t$ distribution for the critical trap number per cell $n_{BD}$ satisfied in a certain soft-breakdown percolation path can be calculated by the existing cell-based percolation model[11,12] with the oxide thinning included:

$$\ln[-\ln(1-F)] = \ln A_{ox} + \ln\left\{ N_t(t_{ox}-2t-t'_{ox}) - \frac{1}{A_0}\ln\left[\sum_{n=0}^{n=n_{BD}-1}\frac{[A_0(t_{ox}-2t-t'_{ox})N_t]^n}{n!}\right]\right\}, \qquad (1)$$

where $F$ denotes the cumulative percentage of time to breakdown. Prior to performing Eq. (1), parameter correlation[15] between $n_{BD}$ and $A_0$ must be taken into account:

$$A_0 = 0.3(t_{ox}-2t-t'_{ox})^2/\sqrt{n_{BD}}. \qquad (2)$$

Equation (2) can readily quantify the area $A_0$ of the localized physically damaged region or percolation path (cell). Equations (1) and (2) can also deal with hard breakdown for $t'_{ox}$

This article is copyrighted as indicated in the article. Reuse of AIP content is subject to the terms at: http://scitation.aip.org/termsconditions. Downloaded to IP: 140.113.38.11 On: Thu, 01 May 2014 07:46:44

$=0$. A unique relationship[13] between the trap density $N_t$ and the electron stress fluence $Q_e$ was employed: $N_t = B\,Q_e^{0.6}$, where $B$ is a constant to be fitted. Thus, the above model with $Q_e = J_G T_{\mathrm{SBD}}$ or $Q_e = J_G T_{\mathrm{HBD}}$ can practically handle time-to-breakdown data with fitting parameters: $B$, $t'_{\mathrm{ox}}$, and $n_{\mathrm{BD}}$.

Best-fitting the model to hard-breakdown data points in Fig. 2 yields $n_{\mathrm{BD}}=4$ and $B=7\times10^{17}\,\mathrm{cm}^{-1.8}\mathrm{C}^{-0.6}$ for two different areas. With known $B$, next fitting soft-breakdown data leads to $n_{\mathrm{BD}}=3$ and $t'_{\mathrm{ox}}=1.0\,\mathrm{nm}$. Adequate reproduction, as shown in Fig. 2, evidences that the statistical distributions of soft breakdown behave intrinsically as hard breakdown.[13,16] The extracted $t'_{\mathrm{ox}}$ is reasonable since its quantity plus the transition-layer thickness $t$ of 0.5 nm is fairly comparable with literature values obtained by $I-V$ fitting: 2.2 nm for the 4 nm gate oxide[2] and a constant of about 1.7 nm over 3.5–5.0 nm gate-oxide thicknesses.[9] On the other hand, the area of the localized physically damaged region was estimated based on Eq. (2) to be 0.3 $\mathrm{nm}^2$, far away from the reported values: i.e., $1.55\times1.55\,\mathrm{nm}^2$ in Ref. 8 and $1\times10^3-6\times10^3\,\mathrm{nm}^2$ in Ref. 9. One of the principal reasons for such order-of-the-magnitude differences is that the direct tunneling depends on the oxide thickness exponentially but on the area only linearly, that is, an adjustment of $t'_{\mathrm{ox}}$ gives rise to an exponential change in tunneling area such as to maintain the same direct tunneling current.

According to the above analysis, the origins of soft and hard breakdown can be clarified in the following: (i) soft breakdown behaves intrinsically as hard breakdown, that is, they share the same defect (neutral trap) generation process and follow Poisson random statistics; (ii) both are independent events corresponding to different $t'_{\mathrm{ox}}$ requirements; and (iii) hard breakdown takes place in a certain path located differently from that for the first soft breakdown. Therefore, hard breakdown can statistically compete with soft breakdown, that is, hard breakdown could dominate making soft breakdown not easily detected. This effect, which can reasonably explain the above-mentioned 5% population for the absence of soft breakdown during stress measurement, has been well documented elsewhere.[18] However, we disagree with the argument of the same citation[18] that soft-breakdown and hard-breakdown phenomena do not obey to the same defect generation kinetics. Instead, more and more evidences[19,20] tends to favor our opinion. Finally, the distinct $t'_{\mathrm{ox}}$ for soft and hard breakdown indicates that the conductance in the former percolation path is lower than the latter, consistent with the recent theory prediction[21] that the upper and lower limits of the conductance stochastic values in the percolation path correspond to the occurrences of hard breakdown and soft breakdown, respectively.

In summary, an oxide thinning cell-based percolation model with parameter correlation has been established to assess soft-breakdown statistics in ultrathin gate oxides. It has exhibited the ability of reproducing the statistical distributions of time to soft breakdown from 3.3-nm-thick oxide samples. Current understandings regarding the origins of soft and hard breakdown, the dimension and area of the localized physically damaged region, and the remaining oxide thickness, have all been substantially improved based on the model.

The authors would like to thank the Advanced Reliability Engineering Department/UMC for the EMMI analysis. Special thanks are devoted to M. J. Chang for performing $C-V$ fitting, and Dr. H. T. Huang and K. N. Yang, Reliability Physics Laboratory, for their stimulating discussions. This work was supported by the National Science Council under Contract No. 89-2215-009-049.

[1] K. Okada, S. Kawasaki, and Y. Hirofuji, Extended Abstracts of the 1994 International Conference on Solid State Devices and Materials (SSDM) (1994), p. 565 (unpublished).
[2] S. H. Lee, B. J. Cho, J. C. Kim, and S. H. Choi, Tech. Dig. Int. Electron Devices Meet. 605 (1994).
[3] T. Yoshida, S. Miyazaki, and M. Hirose, Extended Abstracts of the 1996 International Conference on Solid State Devices and Materials (SSDM) (1996), p. 539 (unpublished).
[4] M. Depas, T. Nigam, and M. M. Heyns, IEEE Trans. Electron Devices **43**, 1499 (1996).
[5] B. E. Weir, P. J. Silverman, D. Monroe, K. S. Krisch, M. A. Alam, G. B. Alers, T. W. Sorsch, G. L. Timp, F. Baumann, C. T. Liu, Y. Ma, and D. Hwang, Tech. Dig. Int. Electron Devices Meet. 73 (1997).
[6] E. Miranda, J. Suñé, R. Rodriguez, M. Nafria, and X. Aymerich, Appl. Phys. Lett. **73**, 490 (1998).
[7] T. Sakura, H. Utsunomiya, Y. Kamakura, and K. Taniguchi, Tech. Dig. Int. Electron Devices Meet. 183 (1998).
[8] D. Z. Y. Ting, Appl. Phys. Lett. **74**, 585 (1999).
[9] W. Mizubayashi, H. Itokawa, S. Miyazaki, and M. Hirose, Extended Abstracts of the 1999 International Conference on Solid State Devices and Materials (SSDM) (1999), p. 318 (unpublished).
[10] Y. D. He, H. Guan, M. F. Li, B. J. Cho, and Z. Dong, Appl. Phys. Lett. **75**, 2432 (1999).
[11] J. Suñé, I. Placencia, N. Barniol, E. Farres, F. Martin, and X. Aymerich, Thin Solid Films **185**, 347 (1990).
[12] D. J. Dumin, J. R. Maddux, R. S. Scott, and R. Subramoniam, IEEE Trans. Electron Devices **41**, 1570 (1994).
[13] R. Degraeve, G. Groeseneken, R. Bellens, M. Depas, and H. E. Maes, Tech. Dig. Int. Electron Devices Meet. 863 (1995).
[14] H. T. Huang, M. J. Chen, J. H. Chen, C. W. Su, C. S. Hou, and M. S. Liang, IEEE International Symposium on VLSI Technology, Systems and Applications, Proceedings of Technical Papers (1999), p. 70 (unpublished).
[15] M. J. Chen, H. T. Huang, J. H. Chen, C. W. Su, C. S. Hou, and M. S. Liang, IEEE Electron Device Lett. **20**, 523 (1999).
[16] E. Y. Wu, E. Nowak, L. K. Han, D. Dufresne, and W. W. Abadeer, Tech. Dig. Int. Electron Devices Meet. 441 (1999).
[17] D. R. Wolters and J. F. Verwey, *Instabilities in Silicon Devices* (Elsevier, Amsterdam, The Netherlands, 1986), p. 332.
[18] S. Bruyere, D. Roy, E. Vincent, and G. Ghibaudo, Microelectron. Reliab. **39**, 815 (1999).
[19] E. Wu, E. Nowak, J. Aitken, W. Abadeer, L. K. Han, and S. Lo, Tech. Dig. Int. Electron Devices Meet. 187 (1998).
[20] J. Suñé, G. Mura, and E. Miranda, IEEE Electron Device Lett. **21**, 167 (2000).
[21] M. A. Alam, B. Weir, J. Bude, P. Silverman, and Don Monroe, Tech. Dig. Int. Electron Devices Meet. 449 (1999).

This article is copyrighted as indicated in the article. Reuse of AIP content is subject to the terms at: http://scitation.aip.org/termsconditions. Downloaded to IP: 140.113.38.11 On: Thu, 01 May 2014 07:46:44